Microfluid Nanofluid (2014) 16:541–551
DOI 10.1007/s10404-013-1252-3

RESEARCH PAPER

Green synthesis of silver nanoparticles-based nanofluids and investigation of their antimicrobial activities

Md. Masud Rahaman Mollick · Biplab Bhowmick · Dipanwita Maity · Dibyendu Mondal · Indranil Roy · Joy Sarkar · Dipak Rana · Krishnendu Acharya · Sanatan Chattopadhyay · Dipankar Chattopadhyay

Received: 6 May 2013 / Accepted: 13 August 2013 / Published online: 25 August 2013

Abstract We have proposed a facile green technique for synthesizing silver nanoparticles-based nanofluids at high temperature and pressure using low molecular weight lactulose solution, which is playing the role of a reducing as well as stabilizing agent. The particle/crystallite sizes, morphology, crystallinity of the nanoparticles are characterized using spectroscopic, microscopic, and diffraction techniques. Since the properties of nanofluids are attractive for technological applications, the investigation of their thermal and electrical conductivities is also immensely important. The material shows a significant enhancement of both thermal and electrical conductivities in comparison to the base fluid due to high surface area, enhanced Brownian motion and layering at the liquid–solid interface of the nanofluids. Moreover, these nanofluids offer excellent antimicrobial activities to different gram class bacteria.

Md. M. R. Mollick · B. Bhowmick · D. Maity · D. Mondal · I. Roy · D. Chattopadhyay (✉)
Department of Polymer Science and Technology, University of Calcutta, 92 A. P. C. Road, Kolkata 700009, India
e-mail: dipankar.chattopadhyay@gmail.com

J. Sarkar · K. Acharya
Molecular and Applied Mycology and Plant Pathology Laboratory, Department of Botany, University of Calcutta, Kolkata, India

D. Rana
Department of Chemical and Biological Engineering, Industrial Membrane Research Institute, University of Ottawa, 161 Louis Pasteur St., Ottawa, ON KIN 6N5, Canada

S. Chattopadhyay
Department of Electronic Science, University of Calcutta, 92 A. P. C. Road, Kolkata 700009, India

Keywords Green synthesis · Lactulose · Silver nanoparticles · Nanofluids · Conductivity · Antimicrobial activity

1 Introduction

Noble metal nanoparticles, with its huge potential applications of ink-jet printing, ammonia sensing, catalytic activities, antimicrobial activity, etc., have attracted a great deal of attractions of the researchers for their interesting and remarkable optical (Joerger et al. 2000), electrical (Magudapathy et al. 2001), catalytic (Jana et al. 1999 and Crooks et al. 2000) sensing (Frederix et al. 2003 and Wu and Meng 2005), etc., properties. Among various noble metal nanoparticles, silver has gained utmost importance for its wide range of application prospects (Carmeron 2009; Karpinski et al. 2000; Liu et al. 2007; Tolaymat et al. 2010) due to unique properties in monodispersed and unagglomerated state. Different existing synthetic methods of preparing noble metal nanostructures namely, electrochemical deposition (Liu and Lin 2004; Sandmann et al. 2000), sol–gel (Saraidarov et al. 2010), micro-emulsion (Andersson et al. 2005), chemical reduction (Bankura et al. 2012; Maity et al. 2011; Petit et al. 1993; Tan et al. 2002; Vorobyova et al. 1999; Yu 2007), have several drawbacks such as high cost, low product yield, uneasiness to control the nanoparticle size, usage of hazardous chemicals, etc. In this context, the development of a greener process for synthesizing such noble metal nanomaterials (Mollick et al. 2012 and Raveendran et al. 2003) would be highly effective and useful. The green method has proven to be better over different conventional approaches owing to its slower kinetics, superior manipulation, and control over crystal growth and their stabilization. Additionally, the green

process is more beneficial over the conventional methods as it is cost-effective and can be easily scaled up for large-scale synthesis.

Nanofluid is basically a nanoscale colloidal suspension of condensed nanomaterials with a number of distinct enhanced thermophysical properties such as thermal conductivity, thermal diffusivity, viscosity, and convective heat transfer co-efficient compared to those of base fluids like oil or water. Manifold increase in thermal conductivity of nanofluids compared to that of base fluid makes these material potentially applicable in micro-electronics, automobiles, power generation, transportation, aerospace, and nuclear power plants (Eastman et al. 2004). In spite of a copious amount of theoretical and experimental studies, an inimitable theory to establish the mechanism of enhancement of thermal conductivity in nanofluids remains intangible. Keblinski et al. (2002) proposed four possible mechanisms for the anomalous increase in thermal conductivity of nanofluids such as Brownian motion of the nanoparticles, molecular-level layering of the liquid at the liquid/particle interface, the augmented heat transport by the nanoparticles and clustering of nanoparticles. There are several reports stating that the microscopic motion (Brownian motion) of the nanoparticles coupled with micro-convective heat transport plays the main role behind the conductivity enhancement in nanofluids (Bhattacharya et al. 2004; Evans et al. 2006; Jang and Choi 2004; Koo and Kleinstreuer 2005; Kumar et al. 2004; Patel et al. 2008; Prasher 2005; Prasher et al. 2006; Shukla and Dhir 2008).

Bulk of the nanofluids are manufactured using most widely known "two-step method," where separately prepared nanoparticles will be dispersed into the base fluid in the second processing step with the help of intensive magnetic force agitation, ultrasonic agitation, high-shear mixing, homogenizing, and ball milling. In this step, nanoparticles may have the propensity to agglomerate due to their high surface area and surface activity and result in an inferior thermal and electrical conductivity of the nanofluids. Therefore, the long-term stability of such nanofluids is an intricate stuff associated with the synthesis technique. Although the use of surfactants in the synthesis of nanofluids restrains the extent of agglomeration, but the functionality of the surfactants for high temperature applications is also a big question. On the contrary, the single-step method seems to show better results in terms of stability and enhanced thermal or electrical conductivity. This process comprises of simultaneously making and dispersing of nanoparticles in the fluid avoiding the tendency of agglomeration. To prepare nanofluids by this technique, several metals such as gold, silver, copper, platinum, etc. have been affirmed because of their catalytic, electric, magnetic, optical, and mechanical properties that are diverse from their counterparts (Lo et al. 2007). Numerous single-step techniques have been grown up to produce nanofluids such as chemical reduction method (Fuentes et al. 2008; Liu et al. 2006; Mishra et al. 2009; Patel et al. 2003; Zhang et al. 2006), pulsed laser ablation technique (Frederix et al. 2003 and Tamjid and Guenther 2010), microwave irradiation (Zhu et al. 2007), submerged arc nanoparticle synthesis system (SANSS) (Lo et al. 2005a, b, 2007), and sputtering on running liquid technique (Tamjid and Guenther 2010).

In the current work, the nanometric silver-dispersed water-based nanofluids via single-step process have been formulated, where a disaccharide, called lactulose, plays the dual role of a reducing as well as a stabilizing mediator. To the best of author's knowledge, it is the first ever report on the synthesis of silver nanofluids using the "green technique." Here, silver nitrate precursor solution is reduced by the lactulose solution and the silver nanoparticles are formed through nucleation and growth, stabilized also by lactulose in order to prepare nanofluid. Lactulose, commercially known as constulose, is a synthetic non-digestible sugar in solution form for oral administration. It is commercially available in liquid form as yellowish odorless clear syrup. It has no taste but exhibits a sweetness equivalent to sucrose. It is basically a disaccharide (double sugar) which is formed from one molecule each of the simple monosaccharides such as fructose and galactose. Commercially, the isomerization of lactose gives lactulose and it is highly water soluble. It is used in the treatment of hepatic encephalopathy, a complication of liver disease and chronic constipation (Lactulose 2013). In the colon, lactulose is broken down primarily to lactic acid and also to small amount of formic acid and acetic acids, by the action of colonic bacteria, which results in an increase in osmotic pressure and slight acidification of the colonic contents (Patil et al. 1987). This in turn causes an increase in stool water content and softness of the stool for movement without any straining. At higher dosage, in pharmaceutical usage, common side effects of lactulose solution are: abdominal cramping, borborygmus, gas, and pungent flatulence that some people find difficult to control in social situations. Excessively high dosage causes explosive, uncontrollable diarrhea, nausea, and vomiting.

The main intention of the study is to achieve a good electrical conductivity of silver nanofluids and in addition, the sufficient stability of nanofluid with controllable silver nanoparticle size. We also observe the effect of precursor concentration on the nanoparticle yield and the conductivity of the nanofluid. The crystallite/particle size, morphology, and the purity of nanoparticles are characterized using microscopic, diffraction, and spectroscopic techniques. Both the enhanced thermal and electrical conductivity with respect to the base fluid have been resolved as a function of concentration and size of silver nanoparticles.

Antimicrobial property being an important feature of silver nanoparticles (Bosetti et al. 2002; Hu et al. 2006; Sarkar et al. 2011), an attempt have also been made to investigate the antimicrobial activity of the synthesized silver nanofluid against various bacteria and it exhibits a great promise as antimicrobial agents as well as its efficacy in the field of medical devices.

2 Experimental

2.1 Materials

Analytical grade silver nitrate ($AgNO_3$) was purchased from Merck (Mumbai, India). Lactulose was obtained from Sigma-Aldrich (98 % pure) and used as received without further purification.

2.2 Preparation of silver nanofluid

Silver nanoparticles were synthesized in base fluid (water). The aqueous solution of lactulose was prepared by dispersing several weight percentages (2, 4, 6, and 8 wt%) of lactulose in the required amount of triple distilled water with continuous stirring until complete dissolution. To investigate the most productive composition to produce the silver nanoparticles using lactulose solution with expected morphology and optimum stability, we started the reaction with an optimal solution of 10^{-3} M $AgNO_3$ and all the above-mentioned lactulose solution individually. $AgNO_3$ solution was mixed drop by drop into 2, 4, 6, and 8 wt% lactulose solution separately for approximately half an hour with vigorous stirring. Separate culture tube of each composition was subjected to put aside in a pressure cooker to initiate the reaction and after the standing time of $\sim$15 min (3rd whistle), the culture tubes were taken out from the pressure cooker. The color change of the colloidal mixture from colorless to yellow demonstrated the formation of silver nanoparticles. Formed silver nanoparticles of each culture tube were analyzed by using UV–Vis spectroscopy and the synthesized silver nanoparticles from the composition of 10^{-3} M $AgNO_3$, and 6 % lactulose showed adequate stability with usual morphology among the four combinations. After that the same synthetic procedure was applied for the silver nanoparticle production with different concentration of $AgNO_3$ (0.0025, 0.004, 0.0055, 0.007, 0.0085, and 0.01 M) using the standard 6 % solution of lactulose.

2.3 Assay for antimicrobial activity of silver nanoparticles against micro-organisms

The silver nanoparticles in sterilized distilled water were tested for their antibacterial activity by the agar diffusion method. Five bacterial strains, *Bacillus subtilis* [MTCC 736], *Bacillus cereus* [MTCC 306], *Pseudomonas aeruginosa* [MTCC 8158], *Staphylococcus aureus* [MTCC 96], and *Escherichia coli* [MTCC 68] along with the silver nitrate solution (10^{-3} M) as a control set were used for this analysis. These bacteria grown on liquid nutrient agar media (HiMedia Laboratories Pvt. Ltd., Mumbai, India) for 24 h prior to the experiment were seeded in agar plates by the pour plate technique. For every bacterial strain, four different cavities were made in one petri plate using a cork borer (10 mm diameter) at more or less equal distance. The cavities were filled with silver nitrate solution (10^{-3} M), 6 wt% of lactulose solution, the silver nanoparticles solution (0.2 mg/ml), and only deionized water, respectively. All the different plates containing the different bacterial strain were incubated at 37 °C for 24 h. Every experiment was repeated for three times.

2.4 UV–Vis absorption spectroscopy analysis

The formation of silver nanoparticles was examined by measuring the UV–Vis spectrum of the reaction medium in the wavelength range from 300 to 700 nm. UV–Vis absorption spectrum of the sample was carried out in an Agilent 8453 Spectrophotometer, USA.

2.5 Dynamic light scattering (DLS) measurement

Dynamic light scattering is also known as photon correlation spectroscopy or quasi-elastic light scattering. This technique is used for determining the particle size distribution and the nature of the particle's motion in the medium. Light scattering technique of the synthesized silver nanoparticles was observed using Zetasizer, Malvern, and Version 6.20.

2.6 Transmission electron microscopy (TEM) measurement

The morphological analysis of the resultant nanoparticles was confirmed by TEM. The sample suspension is drop-casted on a carbon-coated copper grid and the excess solution was removed by tissue paper and allowed to air dry at room temperature overnight. TEM study was monitored on a high-resolution transmission electron microscopic (HRTEM), JEOL JEM 2010 at an accelerating voltage of 200 kV and fitted with a CCD camera.

2.7 X-ray diffraction (XRD) measurement

The crystallinity of synthesized silver nanoparticles was determined and confirmed by XRD analysis. The XRD sample was prepared by depositing the centrifuged sample

on a microscopic glass slide and air-dried overnight. The diffractogram was documented from PANalytical, XPERT-PRO diffractometer using Cu_α ($\lambda = 1.54060$) as X-ray source.

2.8 Electrical conductivity measurement

Nanofluids, due to its electrical conductivity, have got enormous technological importance. To measure the electrical conductivity of nanofluids, DENVER INSTRUMENT MODEL-50, India is employed. Initial calibration was performed using a standard potassium chloride (0.01 mol L^{-1}) solution.

2.9 Thermal conductivity measurement

The transient hot-wire method was employed for measuring the thermal conductivity of nanofluids. The wire serves dual character both as the heat source and the thermometer, and the transient temperature field around the hot wire can be treated as a line source. The hot wire is completely immersed in a vessel containing nanofluid and heat is supplied at a constant rate to measure the necessary temperature rise. This temperature rise depends on the thermal conductivity of the sample through which the wire is inserted. For a given applied heat input (q), the thermal conductivity, k, is calculated from the Fourier's law as:

$$k = \left[\frac{q}{4\pi(T_2 - -T_1)} \ln\left(\frac{t_2}{t_1}\right)\right]$$

where T_1 and T_2 are the temperatures at times t_1 and t_2, respectively. To normalize the possible variation due to human and instrumental errors, the data are expressed as the thermal conductivity ratio with respect to that of the base fluid.

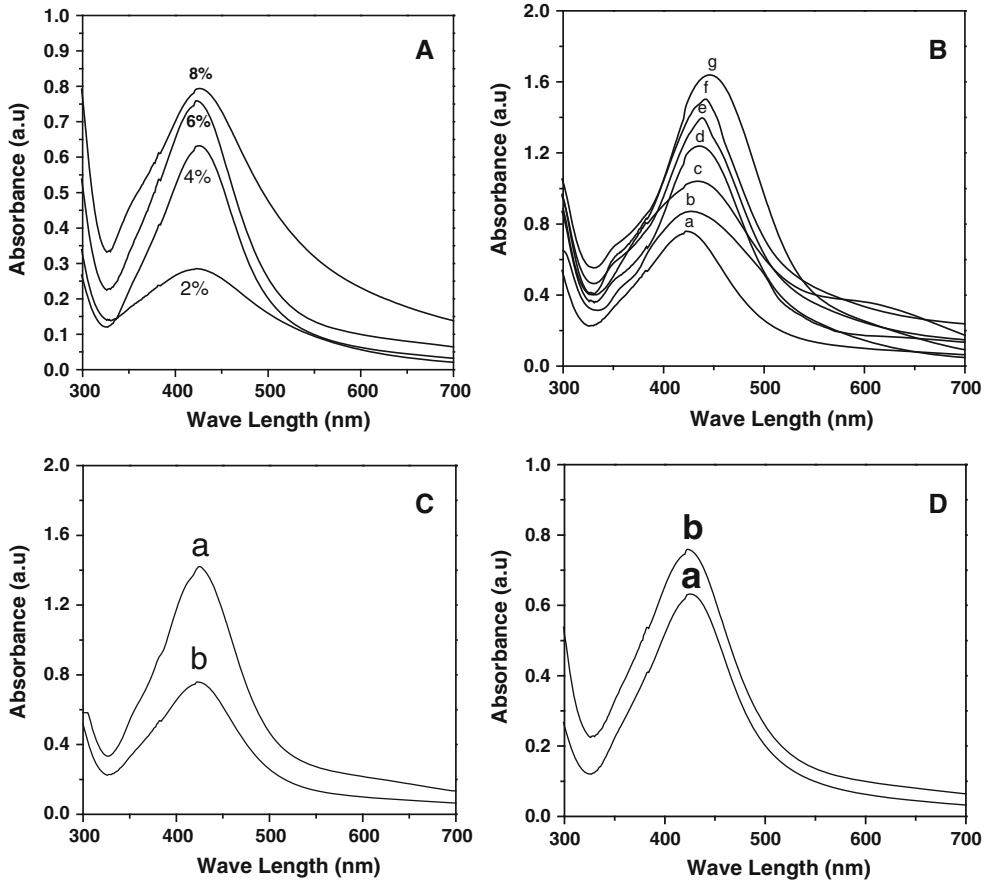

Fig. 1 **A** UV–Vis absorption spectra of silver nanoparticles synthesized (high pressure and temperature) by treating 0.001 M aqueous $AgNO_3$ solution with different lactulose concentration (2, 4, 6, and 8 %). **B** UV–Vis absorption spectra of silver nanoparticles synthesized by treating 6 % lactulose solution with different concentration of aqueous $AgNO_3$ solution (*a*) 0.001 M; (*b*) 0.0025 M; (*c*) 0.0040 M; (*d*) 0.0055 M; (*e*) 0.0070 M; (*f*) 0.0085 M; (*g*) 0.01 M. **C** UV–Vis absorption spectra of (*a*) centrifuged silver nanoparticles re-dispersed in triple distilled water; (*b*) as-synthesized silver nanoparticles using 0.001 M aqueous $AgNO_3$ solution and 6 % lactulose solution. **D** UV–Vis absorption spectra of silver nanoparticles synthesized by treating 0.001 M aqueous $AgNO_3$ solution and 6 % lactulose solution (*a*) after 6 month; (*b*) as prepared

3 Results and discussion

3.1 UV–Vis absorption spectroscopy analysis

UV–Vis spectroscopy is performed to analyze the optical properties of aqueous dispersion of the silver nanoparticle-based nanofluids. It is reported in the literature (Gardea-Torresdey et al. 2003; Sastry et al. 1997; 1998) that the excitation of surface plasmon vibrations of silver nanoparticles appears in the range of 380–450 nm. UV–Vis spectroscopy of synthesized silver nanoparticles using 10^{-3} M $AgNO_3$ with different concentrations of lactulose

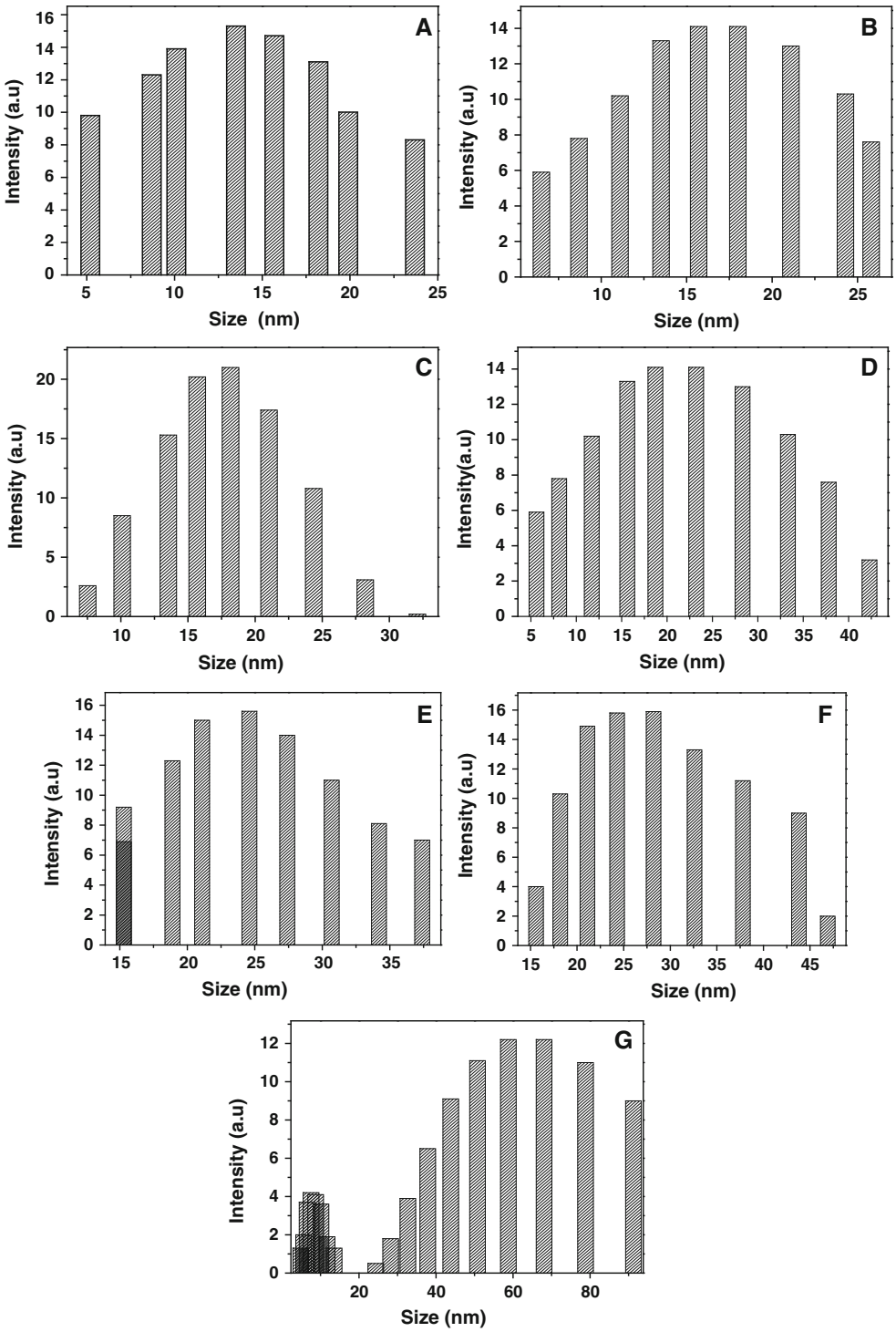

Fig. 2 DLS showing mean average size of silver nanoparticles synthesized (high pressure and temperature) by treating 6 % lactulose solution with different concentrations: **A** 0.001 M; **B** 0.0025 M; **C** 0.0040 M; **D** 0.0055 M; **E** 0.0070 M; **F** 0.0085 M; **G** 0.01 M of aqueous $AgNO_3$ solution

solution is depicted in Fig. 1A. It is clear from Fig. 1A that the absorption band for silver nanoparticle appears in the range of 423–426 nm for different combinations of lactulose solution and 10^{-3} M aqueous solution of $AgNO_3$. It is also observed that the colloidal dispersion of silver nanoparticles synthesized using 6 wt% lactulose solution shows better stability compared to others. So, we further extend our work with 6 wt% lactulose solution as a standard. The synthesis is started with different concentration of $AgNO_3$ solutions (0.001–0.01 M) while standard lactulose solution (6 wt%) is kept intact. Then, the absorption spectra of silver nanoparticles for each composition is taken and presented in Fig. 1B. The absorption band of silver nanoparticles is observed in the range of 423–445 nm for different concentration of $AgNO_3$ and 6 wt% lactulose, which is similar to the earlier report by Wang et al. (2005). The red shift of SPR band of silver nanoparticles to the higher wavelength belongs to the fact that with increasing $AgNO_3$ concentration, a large number of Ag nanoparticles have been produced and to minimize the surface energy, these nanoparticles coalesce with each other to form comparatively large nanoparticles at a faster rate reducing the chances of capping by lactulose molecules. Silver nanoparticles prepared by using different concentrations of $AgNO_3$ solutions show different degree of stability and maximum stability is obtained in case of 10^{-3} M $AgNO_3$. Stability of the colloidal silver nanoparticles, synthesized by using 6 wt% lactulose solution and 10^{-3} M $AgNO_3$ solution, is further confirmed by subsequent ultra-centrifugation and ultra-sonication of the residue in triple distilled water. UV–Vis spectra of re-dispersed silver nanoparticles are recorded and plotted in Fig. 1C. The SPR band at 425 nm is found to be very close to the initial peak, thereby indicating the adequate stability of the synthesized silver nanoparticle-based nanofluids. Furthermore, it is observed after 6 months that the silver nanoparticles-based nanofluid synthesized by using 6 wt% of lactulose solution and 0.001 M $AgNO_3$ solution show the absorption peak at 426 nm (Fig. 1D), which is also very close to the initial peak, indicating almost no agglomeration. So, it can be concluded that the silver nanoparticles in nanofluids are quite stable leading to almost no agglomeration.

3.2 Dynamic light scattering (DLS) measurement

To get the average mean particle size of silver nanoparticles, DLS study of all the compositions comprising of definite concentration of $AgNO_3$ is done and the results are shown in Fig. 2A–G. Comparison of nanoparticle size for every composition is shown in Table 1. It is apparent from Table 1 that the size of silver nanoparticles increases with increasing $AgNO_3$ concentration.

3.3 Transmission electron microscopy (TEM) measurement

To confirm the formation of silver nanoparticles and to inspect its morphology, HRTEM analysis is performed. The TEM image of the as-prepared silver nanoparticles is given in Fig. 3A. It is observed that the silver nanoparticles are mostly spherical in shape with approximate diameter of $\sim$14 nm. The polycrystalline nature of these silver nanoparticles is further evidenced by the selected area electron diffraction pattern with bright circular spots, which is shown in Fig. 3B. In order to analyze the elemental composition of the sample, energy-dispersive spectroscopy (EDS) measurement is performed and the spectrum is shown in Fig. 3C. The strong optical absorption peak at 3 keV in the spectrum indicates the presence of metallic silver nanoparticles.

3.4 X-ray diffraction (XRD) measurement

XRD study is done to further verify the crystalline nature of as-synthesized silver nanoparticles. The XRD pattern of

Table 1 The thermal and electrical conductivities with respect to average silver nanoparticle size synthesized using lactulose and silver nitrate solutions

Concentration of lactulose solution (wt%)	Concentration of $AgNO_3$ solution (M)	Average size of silver nanoparticles (nm)	Electrical conductivity (μS/cm)	Thermal conductivity (mW/m.K)
0	0	0	0	609.5
6	0.001	14	167	611.4
6	0.0025	16	176	615.5
6	0.0040	19	217	629.0
6	0.0055	22	274	664.0
6	0.0070	25	318	685.5
6	0.0085	30	368	688.6
6	0.01	32	433	688.6

the Ag nanoparticles synthesized using 6 wt% lactulose and 0.001(M) $AgNO_3$ solution is displayed in Fig. 4. The diffraction peaks from the (111), (200), (220), and (311) lattice planes are observed at $2\theta = 38.1°$, 44.2°, 64.4°, and 77.6°, respectively. The peaks in the respective XRD patterns are equivalent to the Bragg reflections of face-centered cubic silver and confirm both the identity and purity of the sample. The broadened peaks (full width at half maximum) indicate that the crystallite size of silver lies in the nanometer range. This is further ascertained by the calculation of average crystallite size from the Scherrer formula:

$$d = \frac{0.9\lambda}{\beta \cos\theta}$$

where d is the average crystallite size, λ is the wavelength of radiation, and β is the full width at the half maximum at diffraction angle θ. Using this equation, the calculated crystallite size for silver nanoparticles is found to be $\sim$17 nm at $2\theta = 38.1°$.

3.5 Electrical conductivity and thermal conductivity measurement

The variation of thermal and electrical conductivities with molar concentration of $AgNO_3$ particles is shown in Fig. 5A and the relevant data are presented in Table 1. Since the average particle size has been observed to vary linearly with molar concentration, the variation of both thermal (Paul et al. 2012) and electrical (Solanki and Murthy 2011) conductivities with average particle size would also show the similar trend. It is apparent from the plot in Fig. 5A that the thermal conductivity of nanofluids initially increases slowly up to 611.4 mW/m.K, then rapidly, and finally it saturates to a value of 688.6 mW/m.K for an increase in molar concentration from 0.001 to 0.01 M, and the corresponding variation of average particle size is within the range of 14 to 32 nm. It can be said that the primary phenomenon responsible for such heat conduction in nanofluids is dominated by convection where the concentration and Brownian motion of the constituent

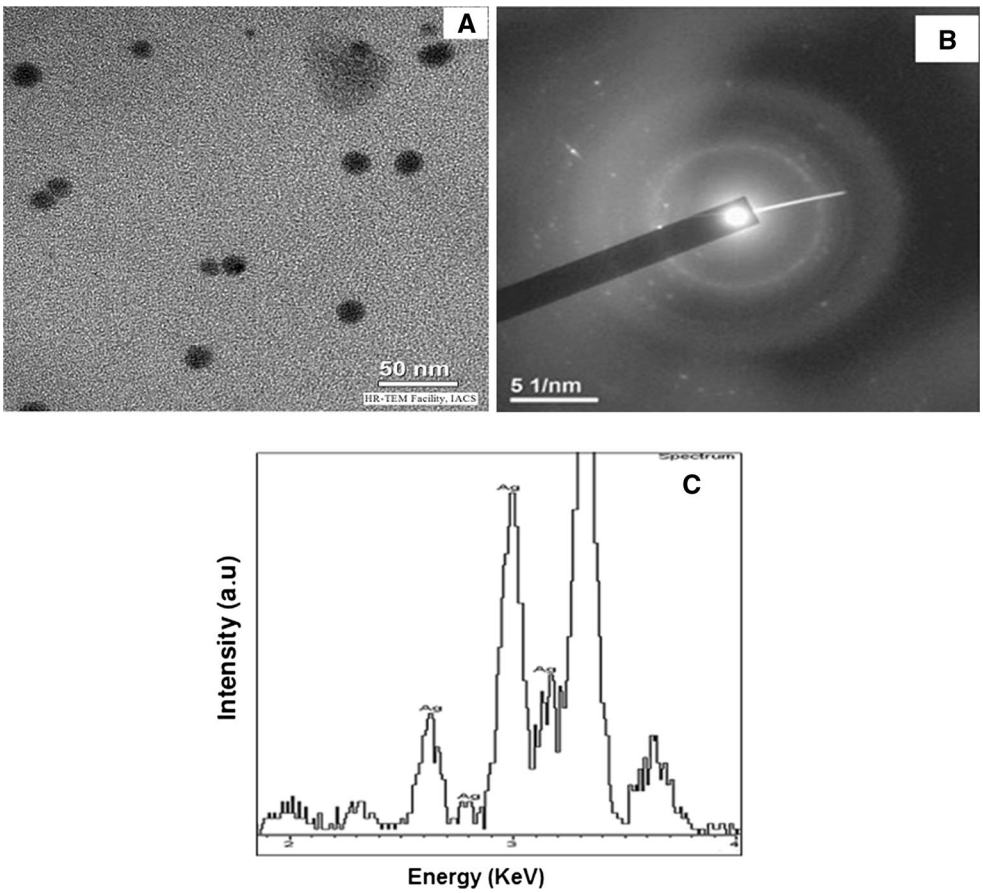

Fig. 3 **A** HRTEM images of Ag nanoparticles synthesized by using 6 % lactulose solution with aqueous 0.001 M $AgNO_3$ solution at high pressure and temperature. **B** SAED pattern of the synthesized silver nanoparticles. **C** Energy-dispersive X-ray spectroscopy (EDS) spectra recorded from silver nanoparticles prepared by lactulose solution at high temperature and pressure

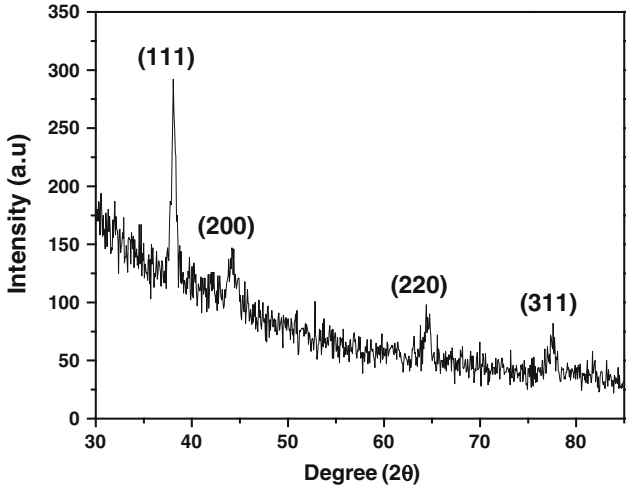

Fig. 4 XRD patterns showing peaks corresponding to the diffraction from (111), (200), (220), and (311) planes of fcc lattice of silver nanoparticles synthesized by using 6 % lactulose solution with aqueous 0.001 M $AgNO_3$ solution at high pressure and temperature

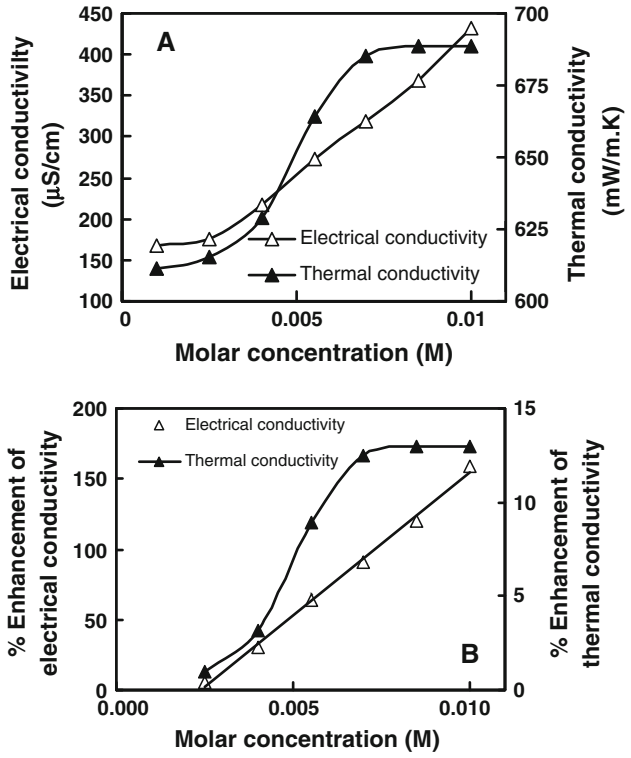

Fig. 5 **A** The plots of variation of thermal and electrical conductivities with molar fraction of silver nitrate and **B** the plots of % enhancement of electrical and thermal conductivities with molar concentration of $AgNO_3$

nanoparticles play a key role. Similarly, the electrical conductivity of the nanofluids initially increases slowly and then it increases rapidly with the increase in $AgNO_3$ concentration as seen in Fig. 5A. Electrical conductivity of the

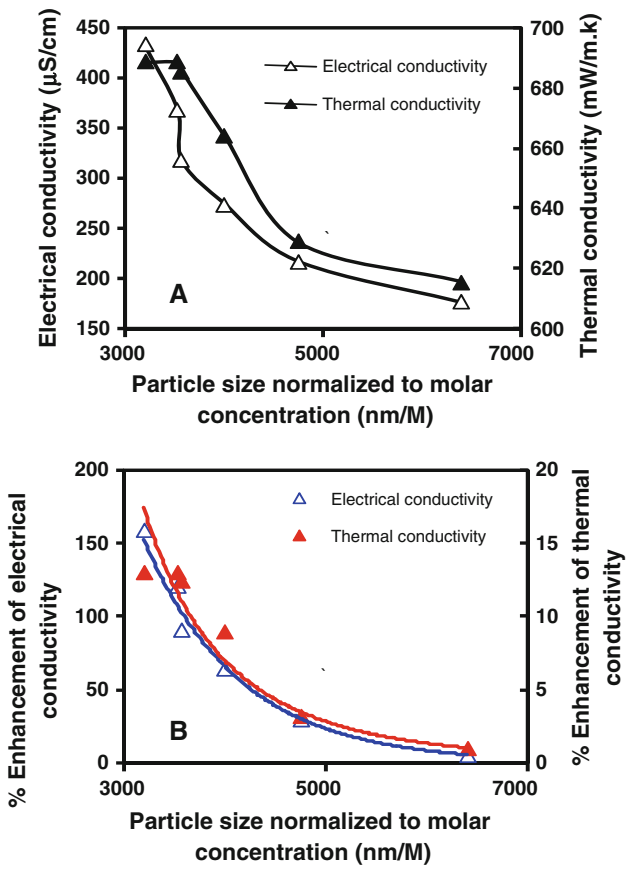

Fig. 6 **A** The plot of variation of thermal and electrical conductivities with the size of Ag nanoparticles normalized to molar concentration and **B** The plots of % enhancement for both electrical and thermal conductivities with the size of silver nanoparticles

nanofluids has been observed to increase from 167 μS/cm for 0.001 M molar concentration to 433 μS/cm for a molar concentration of 0.01.

The percentage of enhancement of electrical and thermal conductivities of nanofluids with molar concentration of $AgNO_3$ is shown in Fig. 5B. The enhancement of electrical and thermal conductivities of nanofluids has been calculated using the following formula:

$$\% \text{ enhancement } = [(E_1 - E_2)/E_1] \times 100$$

where E_1 is the thermal and/or electrical conductivity of nanofluid and E_2 is the thermal and/or electrical conductivity of base fluid. The electrical conductivity enhances almost linearly with molar concentration, whereas the enhancement of thermal conductivity is relatively less for smaller molar concentration. However, the rate of enhancement of thermal conductivity decreases as the molar concentration of $AgNO_3$ increases and finally it saturates for a concentration value of 0.0055 M.

The nanoparticle size has been observed to increase with the increase in $AgNO_3$ concentration in the nanofluids. Therefore, it is difficult to conclude whether the

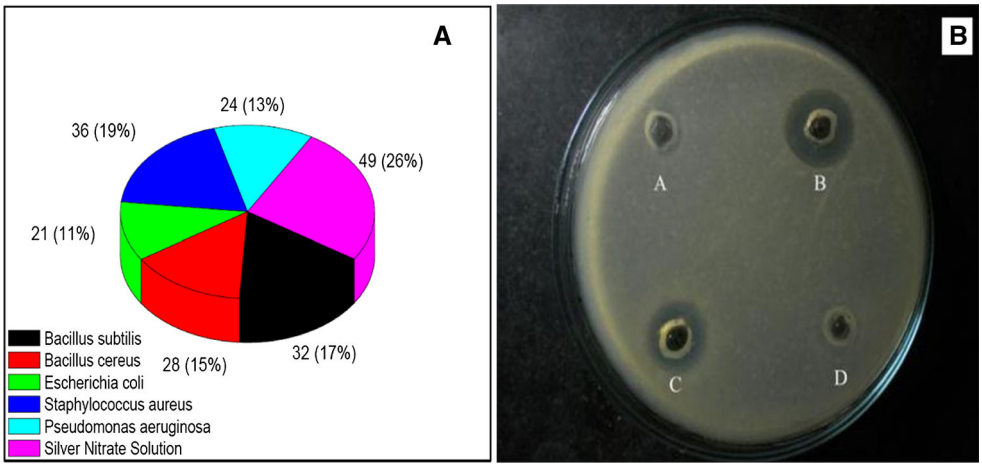

Fig. 7 **A** Radial diameter of inhibitory zone by silver nanoparticle-based nanofluids synthesized by using 6 wt% lactulose solution and 0.001 M $AgNO_3$ solution (0.2 mg/ml) against different Micro-organisms along with the control set (only 10^{-3} M $AgNO_3$ solution). **B** Antibacterial activity of silver nanoparticles assayed by the agar diffusion method in petri plate. Silver nanoparticles poured in the *circular wells* showed the zone of inhibition against *Bacillus subtilis*. The cavities of the petri plate were filled with 6 % lactulose solution (*A*), $AgNO_3$ solution (10^{-3} M) (*B*), silver nanoparticle solution (*C*), and deionized water (*D*), respectively

observations (Fig. 6A, B) are due to the size of the nanoparticles or it is due to the presence of higher number of nanoparticles. In this context, the study of variation of both the thermal and electrical conductivities with average particle size, normalized to molar concentration, will be a superior benchmark since it will show the variation of these important parameters only due to the variation of particle size. Here, the normalized particle size changes from 3,200 to 6,400 nm/M, whereas the $AgNO_3$ concentration is changing from 0.001 to 0.01 M and the measured particle size is in the range of 14 to 32 nm. Such variations are shown in Fig. 6A. It is seen that both the thermal and electrical conductivities decrease in a similar manner with the increase in average particle size normalized to molar concentration. This is attributed to the fact that since the conduction mechanism is controlled by Brownian motion, the higher the particle size higher will be the mass, leading to less amount of heat transfer for the same temperature difference between the terminals. The variation of electrical conductivity is attributed to the reduced surface to volume ratio for the larger particles. The plots of % enhancement for both the electrical and thermal conductivities with normalized particle size have been shown in Fig. 6B. The variation of % enhancement for both the parameters shows a similar exponential nature. The enhancement of electrical conductivity is much higher than that of the thermal conductivity in the particle size range considered. An enhancement as much as 159 % is achieved for a normalized particle size of 3,200 nm/M and minimum enhancement of 5.4 % is achieved for a normalized particle size of 6,400 nm/M, whereas the maximum and minimum enhancement of thermal conductivity of 13 and 1 % are achieved for a normalized particle size of 3,200 and 6,400 nm/M, respectively. As mentioned earlier, the relatively lower enhancement of thermal conductivity is attributed to the fact that it is dominated by Brownian motion where the higher particle size or its higher mass reduces it rapidly, however, the electrical conductivity is related to the surface to volume ratio.

3.6 Antimicrobial activity

The silver nanoparticle-based nanofluids synthesized by using 6 wt% lactulose solution and 0.001 M $AgNO_3$ solution exhibited excellent antibacterial activity against the bacteria, *Bacillus subtilis, Bacillus cereus, Pseudomonas aeruginosa, Staphylococcus aureus*, and *Escherichia coli* by showing the clearing zones around the holes with bacterial growth on petri plates by cup plate method. The radial diameter of the inhibiting zones of *Bacillus subtilis, Bacillus cereus, Escherichia coli, Staphylococcus aureus*, and *Pseudomonas aeruginosa* is 32, 28, 21, 36, and 24 mm, respectively. Silver nanoparticles at the concentration of 0.2 mg/ml showed a range of specificity toward its antimicrobial activity. At the same time, only silver nitrate solution showed a higher range of inhibitory effect in Fig. 7A. The clear inhibition zones were made by silver nitrate solution (B) and silver nanoparticle-based nanofluid solution (C), respectively, against the strain of *Bacillus subtilis* only in Fig. 7B. The clear zone indicated bacterial growth restriction by diffused silver nanoparticles-based nanofluid as well as silver nitrate solution. At the same time, lactulose solution (A) and triple distilled water (D) did not show any inhibition zone in the same figure. Results are mean of three separate experiments, each in triplicate. We have already described earlier in the

introductory section that several silver containing salts showed a good antimicrobial activity. But the higher concentration of silver was harmful to both consumer and microbes. That is why the smaller concentration (nanorange) is much more applicable for usable purpose. This design of silver nanoparticles-based nanofluid synthesis has great potential due to its antibacterial activity. Ag nanoparticles-based nanofluid prepared by the green method described here has great promise as antimicrobial agents. Application of silver nanoparticles-based nanofluid based on these findings may lead to valuable discoveries in various fields such as medical devices and antimicrobial agents.

4 Conclusions

In the present work, a single-step green technique has been developed to synthesize Ag nanoparticle-based nanofluids by using lactulose, which plays both the role of reducing as well as a stabilizing agent. Several important parameters such as distribution of particle sizes, morphology, and purity of the synthesized nanoparticles are characterized by employing microscopic, diffraction, and spectroscopic techniques. The enhanced thermal and electrical conductivities with respect to its base fluids have been studied as a function of concentration and size of silver nanoparticles to investigate its potential application areas. The antimicrobial activities of the silver nanofluids are also investigated.

An absorption band for the silver nanoparticles in the range of 423–426 nm has been observed for different combinations of lactulose and 10^{-3} M $AgNO_3$ solution. A particle size variation of 14–32 nm has been obtained for $AgNO_3$ concentration variation of 0.001–0.01 M. The formation of nanoparticles has also been confirmed from TEM and XRD studies. The variation of molar concentration and consequently resulting particle size shows a huge impact on the thermal and electrical conductivities of the nanofluids. Electrical conductivity has been observed to increase from 167 μS/cm for 0.001 M concentration to 433 μS/cm for a concentration of 0.01 M, thereby almost 159 % enhancement for the particle size variation from 14 to 32 nm. Similarly, a 13 % enhancement has been obtained for the thermal conductivity for the same variation of concentration and particle size. The silver nanoparticle-based nanofluid solution exhibited excellent antibacterial activity against the bacteria, *Bacillus subtilis, Bacillus cereus, Pseudomonas aeruginosa, Staphylococcus aureus*, and *Escherichia coli*. Therefore, the proposed synthesis technique is very useful for developing Ag nanofluids with remarkable thermal, electrical, and antibacterial activities and such properties can be tuned by varying $AgNO_3$ concentration in lactulose.

Acknowledgments The author Md. M. R. Mollick gratefully acknowledge DST, Government of India for providing fellowship under INSPIRE fellowship. D. Maity likes to thank UGC, Government of India for her fellowship. B. Bhowmick wishes to thank the Centre for Nanoscience and Nanotechnology, University of Calcutta, and D. Mondal thanks CSIR, New Delhi for his fellowship. We acknowledge Prof. P. K. Das and G. Paul, Department of Mechanical Engineering, Indian Institute of Technology, Kharagpur, India, for thermal conductivity measurement.

References

Andersson M, Pederson JS, Palmgrist AEC (2005) Silver nanoparticle formation in microemulsions acting both as template and reducing agent. Langmuir 21:11387–11396

Bankura KP, Maity D, Mollick MMR, Mondal D, Bhowmick B, Bain MK, Chakraborty A, Sarkar J, Acharya K, Chattopadhyay D (2012) Synthesis, characterization and antimicrobial activity of dextran stabilized silver nanoparticles in aqueous medium. Carbohydr Polym 89:1159–1165

Bhattacharya P, Saha SK, Yadav A, Phelan PE, Prasher RS (2004) Brownian dynamics simulation to determine the effective thermal conductivity of nanofluids. J Appl Phys 95:6492–6494

Bosetti M, Masse A, Tobin E, Cannas M (2002) Silver coated materials for external fixation devices: in vitro biocompatibility and genotoxicity. Biomaterials 23:887–892

Cameron DS (2009) Chemistry, electrochemistry, and electrochemical applications: Silver. In: Garche J, Dyer CK, Moseley PT, Oguni Z, Rand DAJ, Scrosati B (eds) Encyclopedia of electrochemical power sources. Elsevier, Amsterdam, pp 876–882

Crooks RM, Lemon BI, Sun L, Yeung LK, Zhao M (2000) Dendrimer-encapsulated metals and semiconductors: synthesis, characterization, and applications. Top Curr Chem 212:81–135

Eastman JA, Phillpot SR, Choi SUS, Keblinski P (2004) Thermal transport in nanofluids. Annu Rev Mater Res 34:219–246

Evans W, Fish J, Keblinski P (2006) Role of Brownian motion hydrodynamics on nanofluid thermal conductivity. Appl Phys Lett 88:093116-3

Frederix F, Friedt JM, Choi KH, Laureyn W, Campitelli A, Mondelaers D, Maes G, Borghs G (2003) Biosensing based on light absorption of nanoscaled gold and silver particles. Anal Chem 75:6894–6900

Fuentes RG, Rojas JAP, Jiménez-Pérez JL, Sanchez Ramirez JF, Cruz-Orea A, Mendoza-Alvarez JG (2008) Study of thermal diffusivity of nanofluids with bimetallic nanoparticles with Au(core)/Ag(shell) structure. Appl Surf Sci 255:781–783

Gardea-Torresdey JL, Gomez E, Peralta-Videa JR, Parsons JG, Troiani H, Jose-Yacaman M (2003) Alfalfa sprouts: a natural source for the synthesis of silver nanoparticles. Langmuir 19:1357–1361

Hu Z, Zhang J, Chan WL, Szeto YS (2006) Suspension of silver oxide nanoparticles in chitosan solution and its antibacterial activity in cotton fabrics. Mater Res Soc Symp Proc 920:0920-S02-03(6 pages)

Jana NR, Sau TK, Pal T (1999) Growing small silver particle as redox catalyst. J Phys Chem B 103:115–121

Jang SP, Choi SUS (2004) Role of Brownian motion in the enhanced thermal conductivity of nanofluids. Appl Phys Lett 84:4316–4318

Joerger R, Klaus T, Granqvist CG (2000) Biologically produced silver-carbon composite materials for optically functional thin-film coatings. Adv Mater 12:407–409

Karpinski AP, Russell SJ, Serenyi JR, Murphy JP (2000) Silver based batteries for high power applications. J Power Sources 91:77–82

Keblinski P, Phillpot SR, Choi SUS, Eastman JA (2002) Mechanisms of heat flow in suspensions of nano-sized particles (nanofluids). Int J Heat Mass Transfer 45:855–863

Koo J, Kleinstreuer C (2005) Impact analysis of nanoparticle motion mechanisms on the thermal conductivity of nanofluids. Int Commun Heat Mass 32:1111–1118

Kumar DH, Patel HE, Kumar VRR, Sundararajan T, Pradeep T, Das SK (2004) Model for heat conduction in nanofluids. Phys Rev Lett 93:144301 4 pages

Lactulose (2013) Medline plus drug information, Available at: www.nlm.nih.gov/medlineplus/druginfo/meds/a682338.html, Accessed on: 5 April 2013

Liu YC, Lin LH (2004) New pathway for the synthesis of ultrafine silver nanoparticles from bulk silver substrates in aqueous solutions by sonoelectrochemical methods. Electrochem Commun 6:1163–1168

Liu MS, Lin MCC, Tsai CY, Wang CC (2006) Enhancement of thermal conductivity with Cu for nanofluids using chemical reduction method. Int J Heat Mass Transfer 49:3028–3033

Liu C, Yang X, Yuan H, Zhou Z, Xiao D (2007) Preparation of silver nanoparticle and its application to the determination of ct-DNA. Sensors 7:708–718

Lo CH, Tsung TT, Chen LC, Su CH, Lin HM (2005a) Fabrication of copper oxide nanofluid using submerged arc nanoparticle synthesis system (SANSS). J Nanopart Res 7:313–320

Lo CH, Tsung TT, Chen LC (2005b) Shape-controlled synthesis of Cu-based nanofluid using submerged arc nanoparticle synthesis system (SANSS). J Cryst Growth 277:636–642

Lo CH, Tsung TT, Lin HM (2007) Preparation of silver nanofluid by the submerged arc nanoparticle synthesis system (SANSS). J Alloy Compd 434–435:659–662

Magudapathy P, Gangopadhyay P, Panigrahi BK, Nair KGM, Dhara S (2001) Electrical transport studies of Ag nanoclusters embedded in glass matrix. Phys B 299:142–146

Maity D, Bain MK, Bhowmick B, Sarkar J, Saha S, Acharya K, Chakraborty M, Chattopadhyay D (2011) In situ synthesis, characterization, and antimicrobial activity of silver nanoparticles using water soluble polymer. J Appl Polym Sci 122: 2189–2196

Mishra A, Ram S, Ghosh G (2009) Dynamic light scattering and optical absorption in biological nanofluids of gold nanoparticles in poly(vinyl pyrrolidone) molecules. J Phys Chem C 113:6976–6982

Mollick MMR, Bhowmick B, Maity D, Mondal D, Bain MK, Bankura K, Sarkar J, Rana D, Acharya K, Chattopadhyay D (2012) Green synthesis of silver nanoparticles using *Paederia foetida L.* leaf extract and assessment of their antimicrobial activities. Int J Green Nanotechnol 4:230–239

Patel HE, Das SK, Sundararajan T, Nair AS, George B, Pradeep T (2003) Thermal conductivities of naked and monolayer protected metal nanoparticle based nanofluids: manifestation of anomalous enhancement and chemical effects. Appl Phys Lett 83:2931–2933

Patel HE, Sundararajan T, Das SK (2008) A cell model approach for thermal conductivity of Nanofluids. J Nanopart Res 10:87–97

Patil DH, Westaby D, Mahida YR, Palmer KR, Rees R, Clark ML, Dawson AM, Silk DBA (1987) Comparative modes of action of lactitol and lactulose in the treatment of hepatic encephalopathy. Guit 28:255–259

Paul G, Sarkar S, Pal T, Das PK, Manna I (2012) Concentration and size dependence of nano-silver dispersed water based nanofluids. J Colloid Interface Sci 371:20–27

Petit C, Lixon P, Pileni MP (1993) In situ synthesis of silver nanocluster in AOT reverse micelles. J Phys Chem 97: 12974–12983

Prasher R (2005) Thermal conductivity of nanoscale colloidal solutions (nanofluids). Phys Rev Lett 94:025901 4 pages

Prasher R, Bhattacharya P, Phelan PE (2006) Brownian-motion-based convective-conductive model for the effective thermal conductivity of nanofluids. J Heat Transfer 128:588–595

Raveendran P, Fu J, Wallen SL (2003) Completely "green" synthesis and stabilization of metal nanoparticles. J Am Chem Soc 125:13940–13941

Sandmann G, Dietz H, Plieth W (2000) Preparation of silver nanoparticles on ITO surfaces by a double-pulse method. J Electroanal Chem 491:78–86

Saraidarov T, Levchenko V, Reisfeld R (2010) Synthesis of silver nanoparticles and their stabilization in different sol-gel matrices: optical and structural characterization. Phys Status Solidi C 7:2648–2651

Sarkar J, Saha S, Chattopadhyay D, Patra S, Acharya K (2011) Mycosynthesis of silver nanoparticles and investigation of their antimicrobial activity. J NanoSci NanoEng Appl 1:17–26

Sastry M, Mayya KS, Patil V, Paranjape DV, Hegde SG (1997) Langmuir-Blodgett films of carboxylic acid derivatized silver colloidal particles: role of subphase pH on degree of cluster incorporation. J Phys Chem B 101:4954–4958

Sastry M, Patil V, Sainkar SR (1998) Electrostatically controlled diffusion of carboxylic acid derivatized silver colloidal particles in thermally evaporated fatty amine films. J Phys Chem B 102:1404–1410

Shukla RK, Dhir VK (2008) Effect of Brownian motion on thermal conductivity of nanofluids. J Heat Transfer 130:042406 13 pages

Solanki JN, Murthy ZVP (2011) Preparation of silver nanofluids with high electrical conductivity. J Dispersion Sci Technol 32:724–730

Tamjid E, Guenther BH (2010) Rheology and colloidal structure of silver nanoparticles dispersed in diethylene glycol. Powder Technol 197:49–53

Tan Y, Wang Y, Jiang L, Zhu D (2002) Thiosalicylic acid-functionalized silver nanoparticles synthesized in one-phase system. J Colloid Interface Sci 249:336–345

Tolaymat TM, El Badawy AM, Genaidy A, Scheckel KG, Luxton TP, Suidan M (2010) An evidence-based environmental perspective of manufactured silver nanoparticle in syntheses and applications: a systematic review and critical appraisal of peer-reviewed scientific papers. Sci Total Environ 408:999–1006

Vorobyova SA, Lesnikovich AI, Sobal NS (1999) Preparation of silver nanoparticles by interphase reduction. Colloids Surf A 152:375–379

Wang H, Qiao X, Chen J, Ding S (2005) Preparation of silver nanoparticles by chemical reduction method. Colloids Surf A 256:111–115

Wu S, Meng S (2005) Preparation of ultrafine silver powder using ascorbic acid as reducing agent and its application in MLCI. Mater Chem Phys 89:423–427

Yu DG (2007) Formation of colloidal silver nanoparticles stabilized by Na^+-poly(γ-glutamic acid)-silver nitrate complex via chemical reduction process. Colloids Surf B 59:171–178

Zhang X, Gu H, Fujii M (2006) Effective thermal conductivity and thermal diffusivity of nanofluids containing spherical and cylindrical nanoparticles. J Appl Phys 100:044325

Zhu HT, Zhang CY, Tang YM, Wang JX (2007) Novel synthesis and thermal conductivity of CuO Nanofluid. J Phys Chem C 111:1646–1650